

Involvement of histone H3 phosphorylation through p38 MAPK pathway activation in casticin-induced cytotoxic effects against the human promyelocytic cell line HL-60

HIDETOMO KIKUCHI^{1,2}, BO YUAN^{1,3}, EISUKE YUHARA¹, NORIO TAKAGI³ and HIROO TOYODA¹

¹Department of Clinical Molecular Genetics, School of Pharmacy, Tokyo University of Pharmacy and Life Sciences, Hachioji, Tokyo 192-0392; ²Faculty of Pharmacy, Yasuda Women's University, Asaminami-ku, Hiroshima 731-0153;

³Department of Applied Biochemistry, School of Pharmacy, Tokyo University of Pharmacy and Life Sciences, Hachioji, Tokyo 192-0392, Japan

Received July 13, 2013; Accepted August 26, 2013

DOI: 10.3892/ijo.2013.2106

Abstract. The effect of casticin was investigated by focusing on cell viability, apoptosis induction and cell cycle arrest in HL-60 cells. Casticin induced a dose- and time-dependent decrease in cell viability associated with apoptosis induction and G₂/M cell cycle arrest. The addition of SB203580, an inhibitor for p38 mitogen-activated protein kinase (MAPK), but not SP600125 [c-Jun NH₂-terminal protein kinase (JNK) inhibitor] and PD98059 [extracellular signal-regulated kinase (ERK) inhibitor], abrogated casticin-induced cell cycle arrest and apoptosis associated with the activation of caspases including caspase-8, -9 and -3. Endogenous p38 MAPK activation was observed in untreated cells based on the detection of the expression levels of phospho-p38 MAPK, whereas casticin did not affect the degree of p38 MAPK activation. Interestingly, the addition of SB203580 suppressed casticin-induced phosphorylation of histone H3, a downstream molecule of the p38 MAPK signaling pathway and known to be involved in chromosome condensation during mitosis. More importantly, casticin induced upregulation of intracellular ATP levels. Although casticin induced intracellular reactive oxygen species, antioxidants failed to block casticin-mediated cytotoxicity, indicating that casticin-induced cytotoxicity appears to be independent of reactive oxygen species generation. Based on the fact that SB203580 has been reported to compete with ATP for binding to the active form of p38 MAPK, and consequently blocks the p38 MAPK activity in activating downstream molecules, these

results suggest that casticin induces cytotoxicity associated with apoptosis and cell cycle arrest in HL-60 cells through the p38 MAPK pathway, in which intracellular ATP levels and phosphorylation of histone H3 play critical roles.

Introduction

Cell proliferation is tightly regulated, in which apoptosis plays a key role in the maintenance of homeostasis of normal cells. It has been proposed that dysregulation of apoptosis results in the development of cancer (1). Therefore, the aim of anti-cancer therapy is generally focused on apoptosis induction in premalignant and malignant cells, although other multiple molecular mechanisms such as modulation of carcinogen metabolism, anti-angiogenesis and induction of differentiation are also known to be implicated in its anticancer activity (2,3). So far, two principal signal pathways of apoptosis, such as intrinsic and extrinsic pathways, have been identified (1,2). It has been clarified that activation of caspases including caspase-8, -9 and -3 play critical roles in the initiation and execution of the two signal pathways (2,4). Furthermore, Bid, a pro-apoptotic Bcl-2 family protein is well known to be responsible for the crosstalk between intrinsic and extrinsic pathways (5,6). Besides apoptosis, induction of cell cycle arrest has also been demonstrated to contribute to cytotoxic effects of natural product derived substances (7).

Members of the family of mitogen-activated protein kinases (MAPKs) are involved in apoptotic signaling, as well as in control of growth and differentiation. The MAPKs include p38 kinase, c-Jun NH₂-terminal protein kinase (JNK), and extracellular signal-regulated kinase (ERK) (8). The p38 MAPK and JNK are generally considered to be required for the induction of apoptosis by diverse stimuli (8-11), whereas ERK is usually referred to as a survival mediator involved in the cytoprotective effect (12,13).

Numerous components of edible plants, collectively termed phytochemicals that have beneficial effects for health, are increasingly being reported in scientific literature and these compounds are now widely recognized as potential therapeutic compounds (2,7,14). Natural product derived substances, espe-

Correspondence to: Professor Hiroo Toyoda or Dr Bo Yuan, Department of Clinical Molecular Genetics, School of Pharmacy, Tokyo University of Pharmacy and Life Sciences, 1432-1 Horinouchi, Hachioji, Tokyo 192-0392, Japan
E-mail: toyoda-h@toyaku.ac.jp
E-mail: yuanbo@toyaku.ac.jp

Key words: casticin, apoptosis, G₂/M phase arrest, p38 MAPK, histone H3 phosphorylation; HL-60 cells

cially polyphenolic compounds with very little toxic effects on normal cells, have attracted great attention in therapeutic application in clinical oncology due to their chemopreventive, antitumoral, and chemosensitizing activities against various types of aggressive and recurrent cancers (7, 14,15). Indeed, up to 60% of cancer patients use herbal supplements during and after chemotherapy in the USA (16).

Casticin, a flavonoid, has been demonstrated to show anti-carcinogenic activity in breast cancer cell line MN1 and colonic carcinoma cell line HCT116 (17), as well as epidermoid carcinoma cell line KB (18). We and others have demonstrated that casticin is one of major components of extract from ripe fruit of *Vitex agnus-castus* (Vitex) (19; and Kikuchi *et al* unpublished data). Furthermore, we have demonstrated that Vitex exhibits cytotoxic activities against various types of solid tumor cells, such as KATO-III (gastric signet ring carcinoma cell line), COLO 201 (colon carcinoma cell line) and MCF-7 (breast cancer cell line) (20-22). Although casticin-mediated cytotoxic effects are also demonstrated in leukemia cell lines such as K562, Kasumi-1, HL-60 (23), the precise molecular mechanisms underlying cytotoxic effects of casticin are still needed to be defined in detail. In the present study, the effect of casticin was firstly investigated by focusing on apoptosis induction and cell cycle arrest in HL-60 cells. Next, the details of involvement of MAPK signaling pathways in casticin-mediated cytotoxic effects in HL-60 cells were investigated using MAPK inhibitors.

Materials and methods

Materials. Casticin was obtained from ChromaDex (Irvine, CA, USA). Fetal bovine serum (FBS) was purchased from Nichirei Biosciences (Tokyo, Japan). RPMI-1640 medium, and N-acetyl-L-cysteine (NAC) were obtained from Wako Pure Chemical Industries (Osaka, Japan). Agarose X and dichlorofluorescein diacetate (DCFH-DA) were purchased from Nippon Gene (Tokyo, Japan) and Invitrogen (Carlsbad, CA, USA), respectively. Propidium iodide (PI), ribonuclease A (RNase A), and 2,3-bis(2-methoxy-4-nitro-5-sulfophenyl)-5-((phenylamino)carbonyl)-2H-tetrazolium hydroxide (XTT) were purchased from Sigma-Aldrich (St. Louis, MO, USA). 6-hydroxy-2,5,7,8-tetra-methyl-chroman-carboxylic acid (Trolox), MAPK inhibitors and their negative controls (p38 MAPK inhibitor SB203580 and its negative control SB202474; JNK inhibitor SP600125 and its negative control SP600125NC; ERK inhibitor PD98059) were purchased from Calbiochem (La Jolla, CA, USA).

Cell culture and treatment. HL-60 cells were obtained from the Health Science Research Resources Bank (Tokyo, Japan). Cells were cultured in RPMI-1640 medium supplemented with 10% heat-inactivated FBS and 100 U/ml of penicillin and 100 µg/ml of streptomycin at 37°C in a humidified atmosphere (5% CO₂ in air). Cells were treated with antioxidants, and MAPK inhibitors or their respective negative control, respectively, at the indicated concentrations for 1 h prior to treatment with casticin in the presence or absence of these reagents.

Cell viability assay. After treatment with casticin ranging from 0.1 to 1.0 µg/ml for 24 or 48 h, cell viability was measured

by the XTT assay as described previously (22). IC₅₀ value of casticin was about 0.3 µg/ml calculated from the cell proliferation inhibition curve after 24-h treatment. In order to investigate the effects of antioxidants (NAC and Trolox) and MAP kinase inhibitors on casticin-induced alterations of cell viability, cells were treated with 0.3 µg/ml of casticin in the presence of these reagents for 24-h incubation.

DNA fragmentation analysis. DNA fragmentation analysis was carried out according to a method described previously (24). Briefly, DNA samples (approximately 20 µg DNA/20 µl TE buffer (10 mM Tris-HCl, pH 7.8, 1 mM EDTA)) and 100 bp DNA Ladder were electrophoresed, respectively, on a 2% agarose X gel, and visualized by ethidium bromide staining, followed by viewing under UV Light Printgraph (ATTO Corporation, Tokyo, Japan).

Cell cycle analysis. After treatment with 0.3 µg/ml of casticin in the presence or absence of SB203580 or SB202474 for 12 h, cell cycle analysis was performed using a FACSCanto flow cytometer (Becton-Dickinson, San Diego, CA, USA) according to a method reported previously with modifications (25). With respect to staining cellular DNA, cells were washed twice with PBS, fixed with 1% paraformaldehyde/PBS for 30 min, washed twice again with PBS, permeabilized in 70% (v/v) cold ethanol and kept at -20°C for at least 4 h. Then, cell pellets were washed twice with PBS after centrifugation and incubated with 0.25% Triton X-100 for 5 min on ice. After centrifugation and washing with PBS, cells were resuspended in 500 µl of PI/RNase A/PBS (5 µg/ml of PI and 0.1% RNase A in PBS) and incubated for 30 min in the dark at room temperature. A total of 10,000 events were acquired and Diva software and ModFit LT™ Ver.3.0 (Verity Software House, Topsham, ME, USA) were used to calculate the number of cells at each sub-G₁, G₀/G₁, S and G₂/M phase fraction.

Caspases activity. Activity of caspases was measured using a caspase fluorometric assay kit (BioVision, Mountain View, CA, USA) according to the methods previously reported (26). Briefly, after treatment with 0.3 µg/ml of casticin in the presence or absence of SB203580 or SB202474 for 12 h, cells were washed twice with PBS and suspended in 'cell lysis buffer' from the kit for preparation of cell lysates. Protein amount of 50 µg/50 µl of cell lysates was plated on a 96-well plate, followed by the addition of 50 µl of 2X reaction buffer containing 10 mM DTT to each sample, and then 5 µl of 1 mM caspase substrate (final concentration of 50 µM). After incubation at 37°C for 1 h, fluorescent intensity was measured with a 400 nm excitation filter and 505 nm emission filter using a microplate reader Safire (TECAN, Mannedorf, Switzerland).

Western blot analysis. Protein samples were separated on an SDS-PAGE, followed by transferring to a nitrocellulose membrane as described previously (10). Protein bands were detected using the following primary antibodies: mouse anti-human β-actin (1:5,000 dilution, Sigma-Aldrich); rabbit anti-human phospho-p38 MAPK (Thr180/Tyr182) (1:1,000 dilution), and rabbit anti-human p38 MAPK (1:1,000 dilution) (Cell Signaling Technology, MA, USA). Blotted protein bands

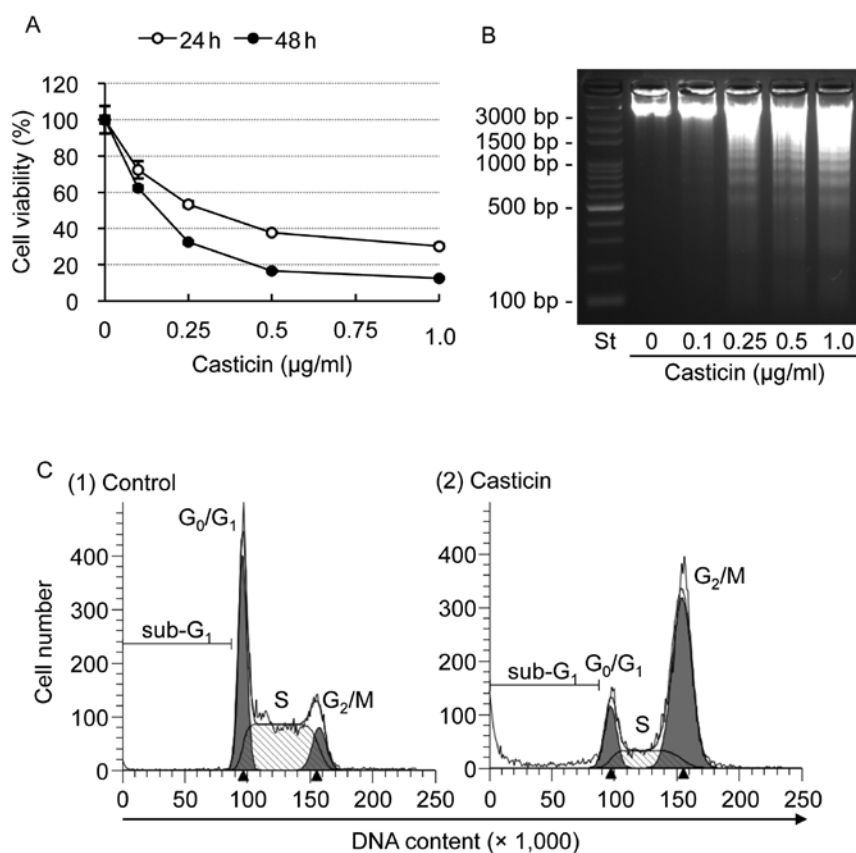


Figure 1. Involvement of apoptosis induction and cell cycle arrest in casticin-induced cytotoxicity in HL-60 cells. (A) Cell viability was determined by XTT assay after the treatment with various concentrations of casticin (0.1, 0.25, 0.5, and 1.0 $\mu\text{g/ml}$) for (○) 24 or (●) 48 h. Relative cell viability was calculated as the ratio of the absorbance at 450 nm of each treatment group against casticin-treated group. Data are shown as the means and SD from three independent experiments. (B) DNA electrophoresis pattern was seen after treatment with indicated concentrations of casticin for 24 h. Lane St shows 100-bp DNA size markers. A representative electrophoretic profile is shown from three independent experiments. (C) After treatment with the IC₅₀ value of casticin at 0.3 $\mu\text{g/ml}$ for 12 h, cell cycle profiling was performed by FACSCanto flow cytometer as described in Materials and methods. Analyzed data and profiles for each sub-G₁, G₀/G₁, S, and G₂/M phase using Diva software and ModFit LT™ ver. 3.0. are shown in the open and the gray area, respectively. Cells at S phase are shown as shaded area. A representative FACS histogram from three separate experiments is shown.

were detected with respective horseradish peroxidase-conjugated secondary antibody and an enhanced chemiluminescence (ECL) western blot analysis system (Amersham Pharmacia Biotech, Buckinghamshire, UK). Relative amounts of the immunoreactive proteins were calculated from the density of the gray level on a digitized image using a program, Multi Gauge Ver. 3.0 (Fujifilm, Tokyo, Japan).

Detection of phosphorylation of histone H3. Similarly to Cell cycle analysis, after treatment with 0.3 $\mu\text{g/ml}$ of casticin in the presence or absence of SB203580 or SB202474 for 12 h, cells were harvested and fixed. Then, cell were suspended in 0.25% Triton X-100 and washed twice with PBS. Next, cell pellets were resuspended in cell staining buffer (140 mM NaCl, 2.7 mM KCl, 10 mM Na₂HPO₄, 1.8 mM KH₂PO₄, 14 mM sodium azide) containing 0.1 μg of anti-histone H3-P mAb conjugated with Alexa Fluor 488 or isotype control conjugated with Alexa Fluor 488 (IgG2a, κ) (BioLegend, San Diego, CA, USA), followed by 2-h incubation in the dark at room temperature. After centrifugation and washing with PBS, cells were resuspended in 500 μl of PI/RNase A/PBS and incubated for 30 min in the dark at room temperature. The expression levels of phosphorylation of histone H3 were

analyzed using a FACSCanto flow cytometer according to a method reported previously (27).

Measurement of intracellular ATP levels. ATP levels were determined using a 'Cellno' ATP assay reagent (TOYO B-Net, Tokyo, Japan) according to the manufacturer's instructions. Briefly, after treatment with 0.3 $\mu\text{g/ml}$ of casticin for 6 h, cells (2×10^5 cells) were washed with PBS twice and suspended in 100 μl of PBS. Cell suspension was inoculated into 96-well microtiter plates followed by the addition of 100 μl of 'Cellno' ATP assay reagent. After shaking for 1 min and incubating for 10 min at room temperature, luminescence was measured in a luminometer.

Measurement of intracellular ROS levels. Intracellular ROS levels were analyzed using DCFH-DA as a ROS-reactive fluorescence probe as described previously (28,29). In brief, after treatment with 0.3 $\mu\text{g/ml}$ of casticin for 3 or 12 h, cells (1×10^6) were suspended in 1 ml of PBS with 5 mM DCFH-DA and incubated for 20 min at 37°C. Next, cells were washed with PBS twice, and resuspended in 500 μl of 2 $\mu\text{g/ml}$ PI/PBS. A total of 30,000 events were acquired for flow cytometry analysis using a FACSCanto flow cytometer and Diva software.

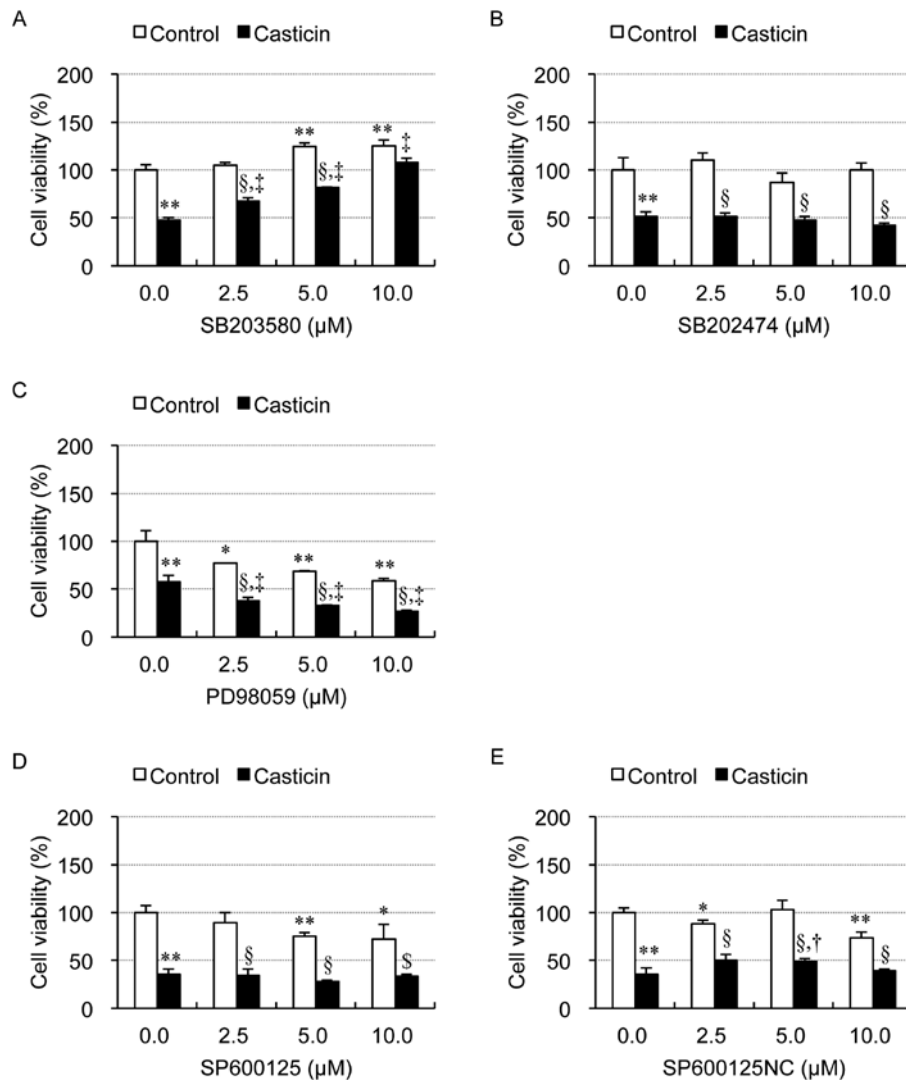


Figure 2. Effect of MAP kinase inhibitors on casticin-induced cytotoxicity in HL-60 cells. Cell viability was determined by XTT assay after treatment with 0.3 $\mu\text{g}/\text{ml}$ of casticin for 24 h in the presence or absence of inhibitors for p38 MAPK, ERK or JNK (2.5, 5.0 and 10.0 μM , respectively). Relative cell viability was calculated as described in Fig. 1. Experiments were carried out in triplicate, and results are shown as mean \pm SD. * $p < 0.05$ and ** $p < 0.01$ vs. control; § $p < 0.05$ and † $p < 0.01$ vs. MAPK inhibitors alone; ‡ $p < 0.05$ and ‡ $p < 0.01$ vs. casticin alone.

Statistical analysis. Data were analyzed using Student's t-test and $p < 0.05$ was considered as statistically significant.

Results

Involvement of apoptosis induction and cell cycle arrest in casticin-induced cytotoxicity in HL-60 cells. A significant decrease in cell viability was observed in a dose- and time-dependent manner in HL-60 cells after treatment with various concentrations of casticin (0.1, 0.25, 0.5 and 1.0 $\mu\text{g}/\text{ml}$) for 24 or 48 h (Fig. 1A). The IC_{50} values were 0.29 ± 0.02 $\mu\text{g}/\text{ml}$ and 0.15 ± 0.002 $\mu\text{g}/\text{ml}$ for 24 and 48 h treatment, respectively, calculated from the respective cell proliferation inhibition curve. A significant difference of the IC_{50} values was observed between two time points ($p < 0.01$). A typical DNA fragmentation ladder representing apoptosis induction was observed at concentrations starting from 0.25 $\mu\text{g}/\text{ml}$ of casticin at 24 h (Fig. 1B), and the extent of fragmentation was more evident at 48 h (data not shown). Consistent with results in Fig. 1B, flow

cytometric analysis showed a significant accumulation of cells in sub- G_1 phase after treatment with the IC_{50} value of casticin at 0.3 $\mu\text{g}/\text{ml}$ for 12 h (Fig. 1C). Concomitantly, G_2/M cell cycle arrest along with a significant decrease in the number of cells both in G_0/G_1 and S phase was also observed (Fig. 1C).

Effects of MAP kinase inhibitors on casticin-induced cytotoxicity in HL-60 cells. The involvement of MAP kinases in casticin-induced cytotoxicity was investigated in HL-60 cells when treated with casticin at 0.3 $\mu\text{g}/\text{ml}$ for 24 h in the presence or absence of inhibitors. Cytotoxicity induced by casticin was significantly abrogated in a dose-dependent manner by the addition of various concentrations (2.5, 5.0 and 10.0 μM) of SB203580, an inhibitor for p38 MAPK, but not by SB202474, a negative control for SB203580 (Fig. 2A and B). However, treatment with even as low as 2.5 μM PD98059, an inhibitor for ERK, not only showed cytotoxicity against HL-60 cells but also enhanced the cytotoxic effect of casticin (Fig. 2C). Moreover, both SP600125, an

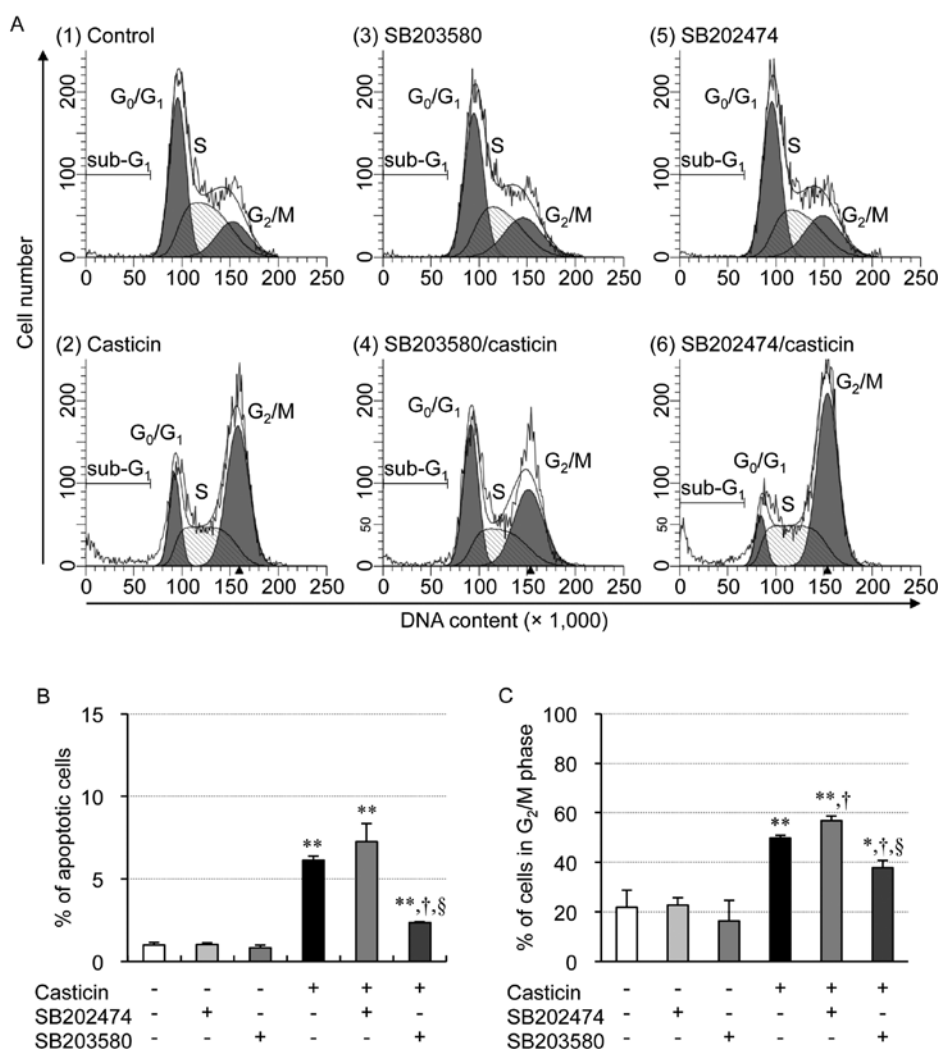


Figure 3. Effect of p38 MAPK inhibitor on casticin-induced apoptosis and cell cycle arrest in HL-60 cells. (A) After the treatment with 0.3 $\mu\text{g/ml}$ of casticin for 12 h in the presence or absence of SB203580 (10 μM) or SB202474 (10 μM), cells were collected and then subjected to flow cytometric analysis. (B and C) Percentage of cells at sub-G₁ and G₂/M phase, respectively, determined as described in Fig. 1. Experiments were carried out in triplicate, and results are shown as mean \pm SD. * $p < 0.05$ and ** $p < 0.01$ vs. control; † $p < 0.01$ vs. casticin alone; § $p < 0.01$ vs. casticin+SB202474.

inhibitor for JNK and its negative control, SP600125NC, appear to show cytotoxic effect against HL-60 cells and little influence on the cytotoxic effect of casticin (Fig. 2D and E).

Effects of p38 MAPK inhibitor on casticin-induced apoptosis and cell cycle arrest in HL-60 cells. After treatment with 0.3 $\mu\text{g/ml}$ of casticin for 12 h, the apoptosis induction and cell cycle arrest were reconfirmed by the increase in the number of cells in sub-G₁, G₂/M phase and the decrease in the number of cells both in G₀/G₁ and S phase, respectively [Fig. 3A (panel 2), B and C]. In contrast, the addition of 10 μM SB203580 not only significantly suppressed the apoptosis induction, but also corrected cell cycle arrest at G₂/M phase, concomitant with an increase in the number of cells in both G₀/G₁ and S phase [Fig. 3A (panel 4), B and C]. The same phenomena were not observed in the presence of SB202474 [Fig. 3A (panel 6), B and C]. Moreover, SB203580 and SB202474 *per se* showed no influence on apoptosis induction and cell cycle arrest in HL-60 cells [Fig. 3A (panels 3 and 5), B and C].

Effects of p38 MAPK inhibitor on casticin-induced caspase activity in HL-60 cells. Given that caspases play crucial roles in apoptosis induction, the activity of caspase-8, -9 and -3 were evaluated in HL-60 cells after treatment with the IC₅₀ value of casticin at 0.3 $\mu\text{g/ml}$ of casticin for 12 h. As expected, caspase-8, -9 and -3 activities showed a significant increase after treatment with casticin (Fig. 4A). Furthermore, their activities were significantly abolished by the addition of 10 μM SB203580, but not by SB202474 (Fig. 4B, C and D). Moreover, SB203580 and SB202474 alone showed no influence on caspase activity.

Detection of phosphorylation of p38 MAPK in casticin-treated HL-60 cells. As shown in Fig. 5, endogenous p38 MAPK activation was observed in untreated HL-60 cells based on the expression levels of phospho-p38 MAPK. Furthermore, no alterations of the expression levels of phospho-p38 MAPK were observed in HL-60 cells treated with 0.3 $\mu\text{g/ml}$ of casticin when compared to those in untreated cells, indicating that treatment with casticin did not affect the degree

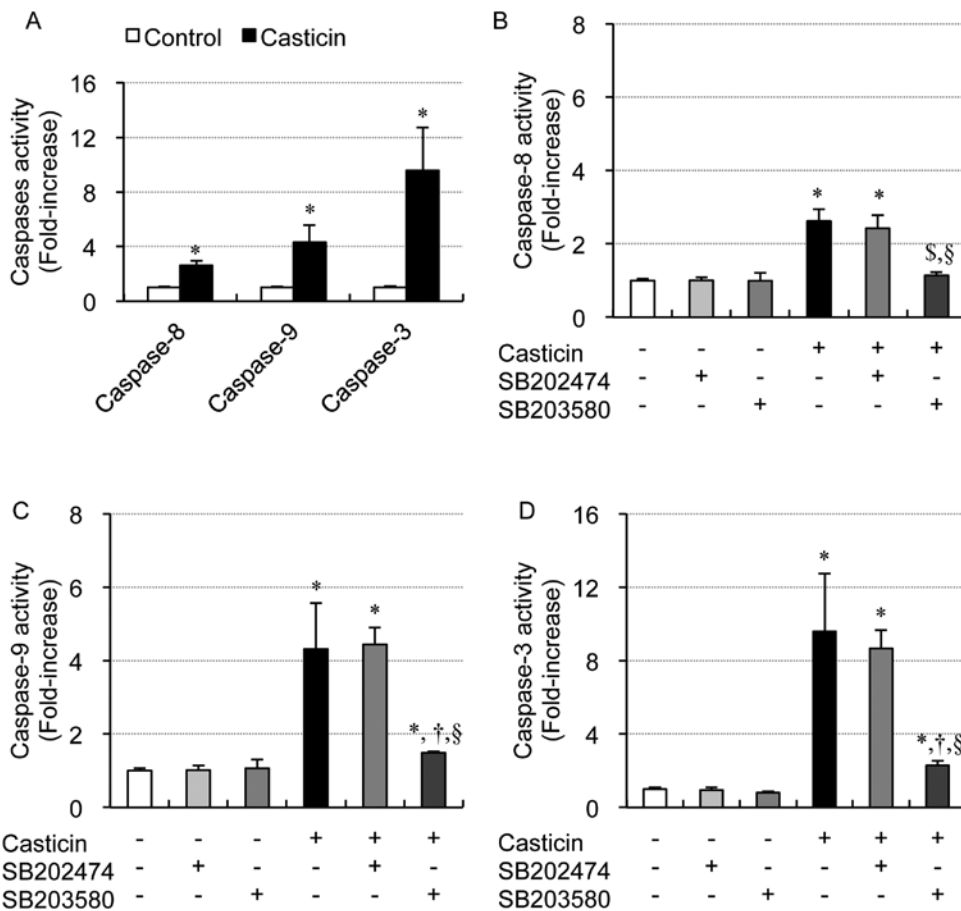


Figure 4. Effect of p38 MAPK inhibitor on casticin-induced caspases activity in HL-60 cells. After the treatment with 0.3 μ g/ml of casticin for 12 h in the presence or absence of SB203580 (10 μ M) or SB202474 (10 μ M), the activity of caspase-8, -9 and -3 was measured using a caspases fluorometric assay kit as described in Materials and methods. Experiments were carried out in triplicate, and results are shown as mean \pm SD. * p <0.01 vs. control; † p <0.05 and § p <0.01 vs. casticin alone; § p <0.01 vs. casticin+SB202474.

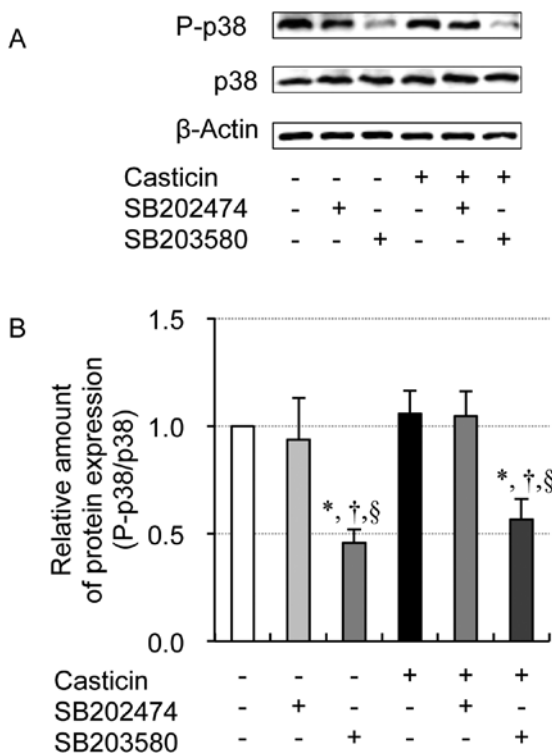


Figure 5. Detection of phosphorylated p38 MAPK in casticin-treated HL-60 cells. (A) After treatment with 0.3 μ g/ml of casticin for 6 h in the presence or absence of SB203580 (10 μ M) or SB202474 (10 μ M), the expression profiles of phospho-p38 MAPK (active form of p38, P-p38), p38 MAPK (total p38) and β -actin proteins were analyzed as described in the text. (B) The expression levels were expressed as the ratios between P-p38 and p38 protein expression levels, and were compared with those at control group. Data are shown as mean \pm SD from three independent experiments. * p <0.01 vs. control; † p <0.01 vs. casticin alone; § p <0.05 vs. casticin+SB202474.

of p38 MAPK activation. Interestingly, the addition of 10 μ M SB203580 significantly inhibited the expression level of phospho-p38 MAPK regardless of the presence or absence of casticin, similar to results in a previous report (9), whereas no such results were observed in the presence of 10 μ M SB202474. It should be noted that there were no changes in the expression levels of total p38 MAPK expression observed in both untreated and treated cells.

Effect of p38 MAPK inhibitor on casticin-induced phosphorylation of histone H3 in HL-60 cells. As shown in Fig. 6A and B, a substantial increase in the expression levels of phospho-histone H3 over the endogenous levels was detected in HL-60 cells treated with 0.3 μ g/ml of casticin

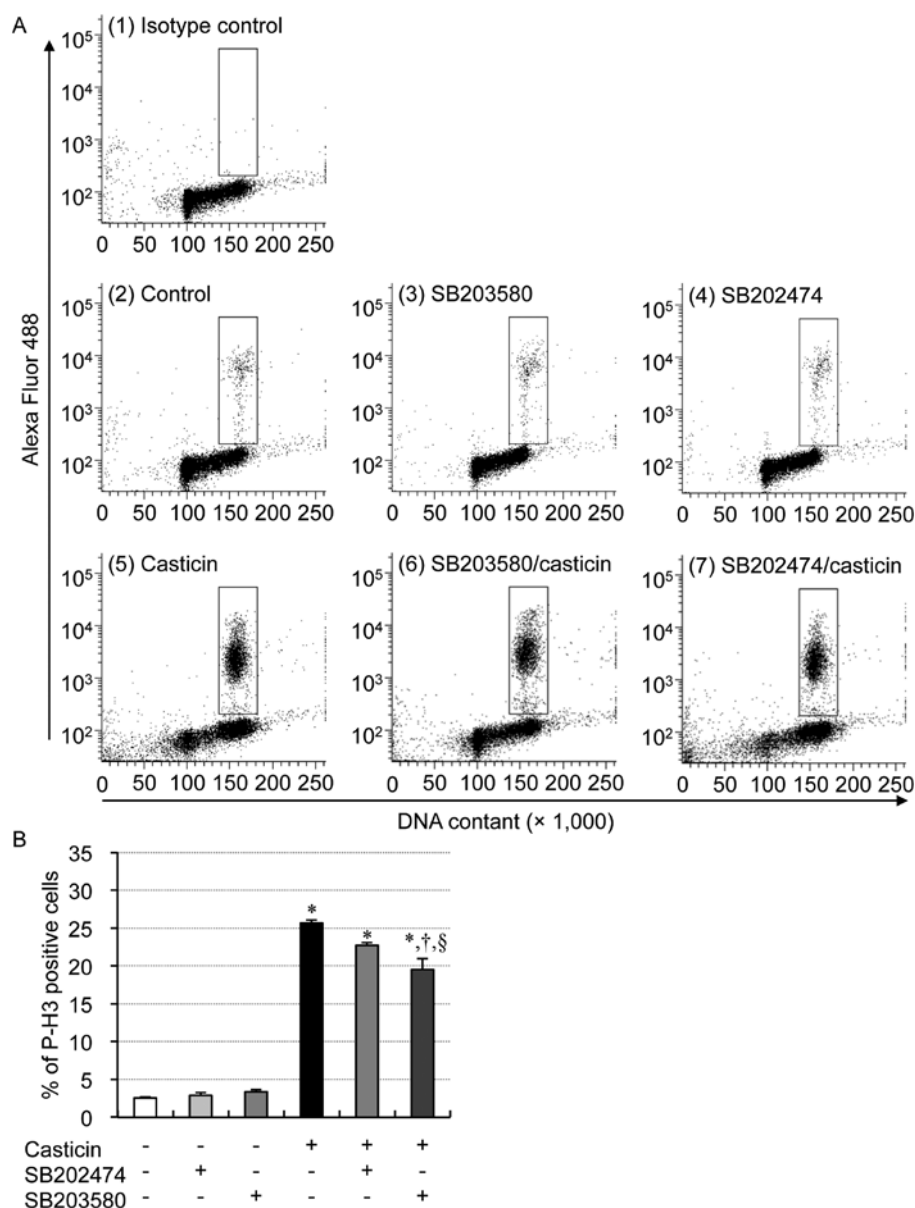


Figure 6. Effect of p38 MAPK inhibitor on casticin-induced phosphorylation of histone H3 in HL-60 cells. (A) After treatment with 0.3 $\mu\text{g/ml}$ of casticin for 12 h in the presence or absence of SB203580 or SB202474 (20 μM , respectively), the phosphorylation of histone H3 (P-H3) in HL-60 cells was analyzed as described in the text. (B) Percentage of P-H3 positive cells is shown. Experiments were carried out in triplicate, and results are shown as the mean \pm SD. * $p < 0.01$ vs. control; † $p < 0.01$ vs. casticin alone; § $p < 0.05$ vs. casticin+SB202474.

for 12 h. The addition of 20 μM SB203580 significantly suppressed casticin-induced phosphorylation of histone H3. Furthermore, the extent of suppression caused by SB203580 was much higher than that by SB202474, although the presence of 20 μM SB202474 also suppressed to some extent the expression level of phospho-histone H3 in HL-60 cells treated with casticin.

Alteration of intracellular ATP level in casticin-treated HL-60 cells. It has been demonstrated that binding of ATP to its binding pocket inside of activated p38 MAPK is a prerequisite step for the activation of downstream molecules of p38 MAPK signaling pathways (30,31). The alteration of intracellular ATP level was thus determined in HL-60 cells after treated with 0.3 $\mu\text{g/ml}$ of casticin for 6 h. As shown in Fig. 7, intercellular

ATP level was significantly upregulated in casticin-treated cells when compared to that in untreated cells.

Alteration of the intracellular reactive oxygen species (ROS) level and effect of antioxidants on casticin-induced cytotoxicity in HL-60 cells. FACS analysis using DCFH-DA as a ROS-reactive fluorescence probe showed a significant time-dependent increase in the intracellular ROS levels after treatment with 0.3 $\mu\text{g/ml}$ of casticin for 3 and 12 h (Fig. 8A). To determine whether the generation of ROS is involved in casticin-induced cytotoxicity, we also investigated the effect of antioxidants such as NAC (2.5-10.0 μM) and Trolox (0.5-1.0 μM). None of these antioxidants blocked the cytotoxicity as assessed by XTT assay indicating that casticin-induced cytotoxicity seems to be independent of ROS generation (Fig. 8B and C).

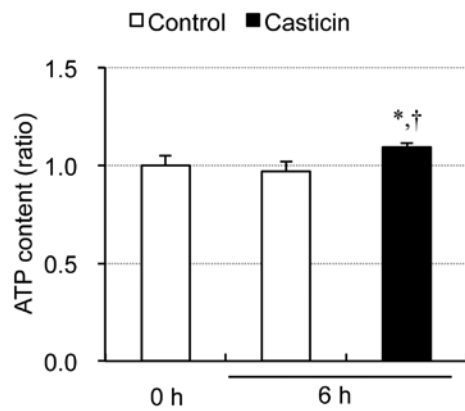


Figure 7. Alteration of intracellular ATP levels in casticin-treated HL-60 cells. After the treatment with $0.3 \mu\text{g/ml}$ of casticin for 6 h, intracellular ATP content was determined as described in the text. Relative amounts were calculated as the ratios of luminescence of treatment group and control at 6-h time point against control at 0-h time point. Experiments were carried out in triplicate, and results are shown as mean \pm SD. * $p < 0.01$ vs. control at 0-h time point; † $p < 0.01$ vs. control at 6-h time point.

Discussion

Results from this study clearly demonstrated that cell viability of HL-60 cells was reduced by casticin in a dose- and time-dependent manner. Furthermore, a dose-dependent

apoptosis induction, along with an accumulation of cells in G_2/M phase and a decrease in the number of cells both in G_0/G_1 and S phase, was observed in the casticin-treated HL-60 cells. A similar effect of casticin was demonstrated in a human colonic carcinoma cell line, HCT116 (17), and epidermoid carcinoma KB cell line (18). Collectively, it is suggested that both apoptosis induction and cell cycle arrest contribute to casticin-induced cytotoxicity. We recently demonstrated that no apparent cytotoxicity of casticin was observed in peripheral blood mononuclear cells from healthy volunteers when treated with concentrations showing significant cytotoxicity in human leukemic cell lines, including HL-60 (Kikuchi *et al.* unpublished data). Similarly, Kobayakawa *et al.*, have shown that KB cells are more sensitive to casticin than human normal fibroblast cells TIG-103 (18). These results thus suggest that casticin possesses selective cytotoxic activity against tumor cells.

We further demonstrated that casticin-induced cytotoxicity was significantly abrogated by the addition of SB203580, an inhibitor for p38 MAPK, in a dose-dependent manner, suggesting that p38 MAPK pathways are involved in the apoptotic induction and cell cycle arrest by casticin treatment. It has been demonstrated that p38 MAPK pathways are involved in apoptosis induction by multiple stimuli in human normal cells as well as cancer cells (9,10). On the other hand, the addition of PD98059, an inhibitor for ERK, did not prevent casticin-induced cytocidal effect against HL-60

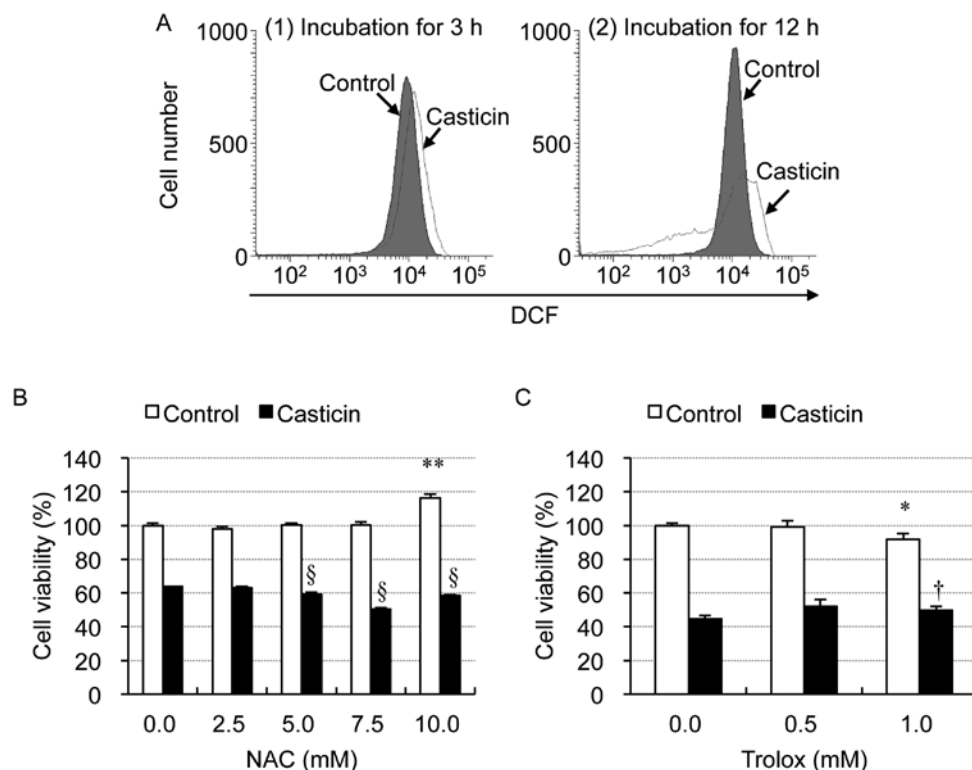


Figure 8. Alteration of the levels of intercellular reactive oxygen species (ROS) and effect of antioxidants on casticin-induced cytotoxicity in HL-60 cells. (A) After treatment with $0.3 \mu\text{g/ml}$ of casticin for 3 or 12 h, cells were incubated with DCFH-DA, a fluorescence probe for ROS, and analyzed by FACSCanto flow cytometer. A representative FACS profile from three separate experiments is shown. (B and C) Cell viability was determined by XTT assay after treatment with $0.3 \mu\text{g/ml}$ of casticin for 24 h in the presence or absence of NAC (2.5, 5.0, 7.5 and 10.0 mM) and Trolox (0.5 and 1.0 mM), respectively. Relative cell viability was calculated as described in Fig. 1. Experiments were carried out in triplicate, and results are shown as the mean \pm SD. * $p < 0.05$ and ** $p < 0.01$ vs. control; † $p < 0.05$ and ‡ $p < 0.01$ vs. casticin alone.

cells, and conversely enhanced the cytotoxic effect, in agreement with previous studies showing that ERK activation exerts a cytoprotective effect against various stimuli (12,13). Although the JNK has generally been associated with proapoptotic actions and growth inhibitory signals (8), here we demonstrated that the treatment with SP600125, an inhibitor for JNK, appears to show slight cytotoxic effect against HL-60 cells and little influence on the cytotoxic effect of casticin. In this regard, previous reports have demonstrated that JNK can be a prosurvival signal for the growth of hepatocellular carcinoma cells (32) and gastrointestinal cancer cell lines (33). Taking these previous results and our observations into account, we suggest that differential role of MAPKs in cellular responses is dependent on cell types, and that p38 MAPK, rather than ERK or JNK, plays a critical role in casticin-induced cytotoxicity in HL-60 cells.

Our results further demonstrated that the addition of SB203580 clearly corrected casticin-induced cell cycle arrest at G₂/M phase, concomitant with an increase in the number of cells in both G₀/G₁ and S phase. Furthermore, the activation of caspases including caspase-8, -9 and -3, which are key players in two principal signal pathways of apoptosis such as intrinsic and extrinsic pathways (2,4), was significantly abolished by the addition of SB203580. In this regard, it should be noted that dihydroartemisin (DHA) effectively induced p38 MAPK activation along with apoptosis in HL-60 cells, which was accompanied by caspase activation (11). Furthermore, pretreatment with SB203580 reversed DHA-induced caspase activation and consequently abrogate the apoptosis induction (11). Taken together, we propose that p38 MAPK activation function upstream of caspase activation in casticin-induced apoptosis in HL-60 cells. We have previously demonstrated that crosstalk between intrinsic and extrinsic pathways via Bid activation plays a critical role in apoptosis induction of KATO-III when treated with Vitex (21), in which casticin is one of the major components (19). Experiments focusing on the activation of Bid are needed to clarify the relationship between intrinsic and extrinsic pathways.

Although no alteration of the expression level of phospho-p38 MAPK was observed in HL-60 cells treated with casticin, a substantial increase in the expression levels of phospho-histone H3 over the endogenous levels was detected. Phosphorylation of histone H3 has long been implicated in chromosome condensation during mitosis (34,35). It should be noted that histone H3 phosphorylation is implicated in an oxidant-induced DNA damage and cell death in renal proximal tubular epithelial cells (36). Furthermore, Waring *et al* reported that fungal gliotoxin induce phosphorylation of histone H3 along with apoptosis in mouse thymocytes, and further demonstrated that the levels of apoptosis correlated with degree of histone H3 phosphorylation (37). Collectively, we suggest that phosphorylation of histone H3 plays a critical role in the casticin-induced cytotoxicity in HL-60 cells.

We demonstrated that the addition of SB203580 significantly suppressed casticin-induced phosphorylation of histone H3. It has been demonstrated that in response to various stimuli, activated p38 MAPK regulates the immediate early gene expression and other cellular responses by phosphorylating various substrates, including chromatin proteins, and transcription factors (38,39). Therefore, casticin-triggered

phosphorylation of histone H3 is suggested to be mediated by the p38 MAPK pathway. However, the fact that treatment with casticin did not alter the expression level of phospho-p38 MAPK raised a question of how casticin activates the p38 MAPK pathway including its downstream molecules such as histone H3. To address this, we investigated intracellular ATP levels in casticin-treated HL-60 cells, since binding of ATP to its binding pocket inside of activated p38 MAPK has been reported to be required for the activation of downstream molecules of p38 MAPK (30,31). As expected, intracellular ATP levels were significantly upregulated in casticin-treated cells when compared to those in untreated cells. It has also been demonstrated that SB203580 has been reported to compete with ATP for binding to the active form of p38 MAPK, and consequently blocks the p38 MAPK activity in activating downstream molecules such as MAPK-activated protein kinase 2 and activating transcription factor 2 (31,40). Therefore, the fact that the inhibition of casticin-induced phosphorylation of histone H3 caused by SB203580 might be attributed to the competition of SB203580 with ATP. Indeed, phosphorylation of histone H3 induced by cisplatin and arsenite has been demonstrated to be mediated by p38 MAPK pathway in HeLa cells and mouse embryo fibroblasts, respectively, since the addition of p38 MAPK inhibitor blocked phosphorylation of histone H3 (41,42).

We have previously demonstrated that oxidative stress is implicated in KATO-III cell apoptosis induced by Vitex (21), but not in COLO 201 cells (26). These results suggest a cell-type dependent apoptosis induction by oxidative stress. In the current study, although reactive oxygen species (ROS) increased in response to casticin, ROS did not seem to play a pivotal role in the apoptotic process since different antioxidants were unable to provide cell protection. These results thus suggest that casticin-induced cytotoxicity in HL-60 cells might be mediated through a mechanism independent of ROS generation.

In conclusion, we demonstrated that apoptosis and cell cycle arrest are involved in casticin-induced cytotoxicity in HL-60 cells, and that both intrinsic and extrinsic pathway seem to be involved in induction of apoptosis. We also demonstrated for the first time that the addition of SB203580 not only abrogated apoptosis induction but also correct cell cycle arrest caused by casticin, suggesting p38 MAPK pathway plays a pivotal role in casticin-induced cytotoxicity. We further demonstrated that a substantial increase in the expression levels of phospho-histone H3, along with intracellular ATP levels was observed in HL-60 cells after treatment with casticin. More importantly, the addition of SB203580 significantly suppressed casticin-induced phosphorylation of histone H3. Since SB203580 has been reported to compete with ATP for binding to the active form of p38 MAPK, and that it consequently blocks the p38 MAPK activity in downstream molecules including histone H3, we suggest that casticin-induced cytotoxicity is associated with apoptosis and cell cycle arrest in HL-60 cells through p38 MAPK pathway, in which intracellular ATP level and phosphorylation of histone H3 play critical roles. Collectively, these results suggest that casticin could possess a strong potential as a therapeutic agent for cancer treatment.

Acknowledgements

This study was supported in part by grants from the Ministry of Education, Culture, Sports, Science and Technology and by the Promotion and Mutual Aid Corporation for Private Schools of Japan. The authors thank Mr. Yoshiro Namai, Managing Director BioLegend Japan KK, for advice on cell cycle analysis and providing anti-histone H3-P mAb.

References

1. Indran IR, Tufo G, Pervaiz S and Brenner C: Recent advances in apoptosis, mitochondria and drug resistance in cancer cells. *Biochim Biophys Acta* 1807: 735-745, 2011.
2. Yuan B, Yoshino Y, Kaise T and Toyoda H: Application of arsenic trioxide therapy for patients with leukemia. In: *Biological Chemistry of Arsenic*. Antimony and Bismuth. Sun H (ed). John Wiley & Sons Ltd., Chichester, pp263-292, 2011.
3. Wang ZY and Chen Z: Acute promyelocytic leukemia: from highly fatal to highly curable. *Blood* 111: 2505-2515, 2008.
4. Ryter SW, Kim HP, Hoetzel A, Park JW, Nakahira K, Wang X and Choi AM: Mechanisms of cell death in oxidative stress. *Antioxid Redox Signal* 9: 49-89, 2007.
5. Kantari C and Walczak H: Caspase-8 and bid: caught in the act between death receptors and mitochondria. *Biochim Biophys Acta* 1813: 558-563, 2011.
6. Viswanath V, Wu Y, Boonplueang R, Chen S, Stevenson FF, Yantiri F, Yang L, Beal MF and Andersen JK: Caspase-9 activation results in downstream caspase-8 activation and bid cleavage in 1-methyl-4-phenyl-1,2,3,6-tetrahydropyridine-induced Parkinson's disease. *J Neurosci* 21: 9519-9528, 2001.
7. Reddy L, Odhav B and Bhoola KD: Natural products for cancer prevention: a global perspective. *Pharmacol Ther* 99: 1-13, 2003.
8. Cargnello M and Roux PP: Activation and function of the MAPKs and their substrates, the MAPK-activated protein kinases. *Microbiol Mol Biol Rev* 75: 50-83, 2011.
9. Zhuang S, Demirs JT and Kochevar IE: p38 mitogen-activated protein kinase mediates bid cleavage, mitochondrial dysfunction, and caspase-3 activation during apoptosis induced by singlet oxygen but not by hydrogen peroxide. *J Biol Chem* 275: 25939-25948, 2000.
10. Yuan B, Ohyama K, Takeichi M and Toyoda H: Direct contribution of inducible nitric oxide synthase expression to apoptosis induction in primary smooth chorion trophoblast cells of human fetal membrane tissues. *Int J Biochem Cell Biol* 41: 1062-1069, 2009.
11. Lu JJ, Meng LH, Cai YJ, Chen Q, Tong LJ, Lin LP and Ding J: Dihydroartemisinin induces apoptosis in HL-60 leukemia cells dependent of iron and p38 mitogen-activated protein kinase activation but independent of reactive oxygen species. *Cancer Biol Ther* 7: 1017-1023, 2008.
12. Milella M, Kornblau SM, Estrov Z, Carter BZ, Lapillonne H, Harris D, Konopleva M, Zhao S, Estey E and Andreeff M: Therapeutic targeting of the MEK/MAPK signal transduction module in acute myeloid leukemia. *J Clin Invest* 108: 851-859, 2001.
13. Yao J, Qian CJ, Ye B, Zhang X and Liang Y: ERK inhibition enhances TSA-induced gastric cancer cell apoptosis via NF- κ B-dependent and Notch-independent mechanism. *Life Sci* 91: 186-193, 2012.
14. Yuan B, Imai M, Kikuchi H, Fukushima S, Hazama S, Akaike T, Yoshino Y, Ohyama K, Hu X, Pei X, Toyoda H: Cytocidal effects of polyphenolic compounds, alone or in combination with, anticancer drugs against cancer cells: Potential future application of the combinatory therapy. In: *Apoptosis and Medicine*. Ntuli TM (ed). InTech, Rijeka, pp155-174, 2012.
15. Imai M, Kikuchi H, Yuan B, Aihara Y, Mizokuchi A, Ohyama K, Hirobe C and Toyoda H: Enhanced growth inhibitory effect of 5-fluorouracil in combination with *Vitex agnus-castus* fruits extract against a human colon adenocarcinoma cell line, COLO 201. *J Chin Clin Med* 6: 14-19, 2011.
16. Cassileth B, Yeung KS and Gubili J: Herbs and other botanicals in cancer patient care. *Curr Treat Options Oncol* 9: 109-116, 2008.
17. Haïdara K, Zamir L, Shi QW and Batist G: The flavonoid Casticin has multiple mechanisms of tumor cytotoxicity action. *Cancer Lett* 242: 180-190, 2006.
18. Kobayakawa J, Sato-Nishimori F, Moriyasu M and Matsukawa Y: G2-M arrest and antimetabolic activity mediated by casticin, a flavonoid isolated from *Vitex Fructus* (*Vitex rotundifolia* Linne fil.). *Cancer Lett* 208: 59-64, 2004.
19. Chen SN, Friesen JB, Webster D, Nikolic D, van Breemen RB, Wang ZJ, Fong HH, Farnsworth NR and Pauli GF: Phytoconstituents from *Vitex agnus-castus* fruits. *Fitoterapia* 82: 528-533, 2011.
20. Ohyama K, Akaike T, Hirobe C and Yamakawa T: Cytotoxicity and apoptotic inducibility of *Vitex agnus-castus* fruit extract in cultured human normal and cancer cells and effect on growth. *Biol Pharm Bull* 26: 10-18, 2003.
21. Ohyama K, Akaike T, Imai M, Toyoda H, Hirobe C and Bessho T: Human gastric signet ring carcinoma (KATO-III) cell apoptosis induced by *Vitex agnus-castus* fruit extract through intracellular oxidative stress. *Int J Biochem Cell Biol* 37: 1496-1510, 2005.
22. Imai M, Kikuchi H, Denda T, Ohyama K, Hirobe C and Toyoda H: Cytotoxic effects of flavonoids against a human colon cancer derived cell line, COLO 201: a potential natural anti-cancer substance. *Cancer Lett* 276: 74-80, 2009.
23. Shen JK, Du HP, Yang M, Wang YG and Jin J: Casticin induces leukemic cell death through apoptosis and mitotic catastrophe. *Ann Hematol* 88: 743-752, 2009.
24. Yuan B, Ohyama K, Bessho T, Uchide N and Toyoda H: Imbalance between ROS production and elimination results in apoptosis induction in primary smooth chorion trophoblast cells prepared from human fetal membrane tissues. *Life Sci* 82: 623-630, 2008.
25. Darzynkiewicz Z, Bruno S, Del Bino G, Gorczyca W, Hotz MA, Lassota P and Traganos F: Features of apoptotic cells measured by flow cytometry. *Cytometry* 13: 795-808, 1992.
26. Imai M, Yuan B, Kikuchi H, Saito M, Ohyama K, Hirobe C, Oshima T, Hosoya T, Morita H and Toyoda H: Growth inhibition of a human colon carcinoma cell, COLO 201, by a natural product, *Vitex agnus-castus* fruits extract, in vivo and in vitro. *Adv Biol Chem* 2: 20-28, 2012.
27. Ozawa K: Reduction of phosphorylated histone H3 serine 10 and serine 28 cell cycle marker intensities after DNA damage. *Cytometry A* 73: 517-527, 2008.
28. Robinson JP, Bruner LH, Bassoe CF, Hudson JL, Ward PA and Phan SH: Measurement of intracellular fluorescence of human monocytes relative to oxidative metabolism. *J Leukoc Biol* 43: 304-310, 1988.
29. Uchide N, Ohyama K, Bessho T, Yuan B and Yamakawa T: Effect of antioxidants on apoptosis induced by influenza virus infection: inhibition of viral gene replication and transcription with pyrrolidine dithiocarbamate. *Antiviral Res* 56: 207-217, 2002.
30. Frantz B, Klatt P, Pang M, Parsons J, Rolando A, Williams H, Tocci MJ, O'Keefe SJ and O'Neill EA: The activation state of p38 mitogen-activated protein kinase determines the efficiency of ATP competition for pyridinylimidazole inhibitor binding. *Biochemistry* 37: 13846-13853, 1998.
31. Young PR, McLaughlin MM, Kumar S, Kassis S, Doyle ML, McNulty D, Gallagher TF, Fisher S, McDonnell PC, Carr SA, Huddleston MJ, Seibel G, Porter TG, Livi GP, Adams JL and Lee JC: Pyridinyl imidazole inhibitors of p38 mitogen-activated protein kinase bind in the ATP site. *J Biol Chem* 272: 12116-12121, 1997.
32. Kuntzen C, Sonuc N, De Toni EN, Opelz C, Mucha SR, Gerbes AL and Eichhorst ST: Inhibition of c-Jun-N-terminal-kinase sensitizes tumor cells to CD95-induced apoptosis and induces G2/M cell cycle arrest. *Cancer Res* 65: 6780-6788, 2005.
33. Xia HH, He H, De Wang J, Gu Q, Lin MC, Zou B, Yu LF, Sun YW, Chan AO, Kung HF and Wong BC: Induction of apoptosis and cell cycle arrest by a specific c-Jun NH2-terminal kinase (JNK) inhibitor, SP-600125, in gastrointestinal cancers. *Cancer Lett* 241: 268-274, 2006.
34. Zhong S, Goto H, Inagaki M and Dong Z: Phosphorylation at serine 28 and acetylation at lysine 9 of histone H3 induced by trichostatin A. *Oncogene* 22: 5291-5297, 2003.
35. Goto H, Tomono Y, Ajiro K, Kosako H, Fujita M, Sakurai M, Okawa K, Iwamatsu A, Okigaki T, Takahashi T and Inagaki M: Identification of a novel phosphorylation site on histone H3 coupled with mitotic chromosome condensation. *J Biol Chem* 274: 25543-25549, 1999.

36. Tikoo K, Lau SS and Monks TJ: Histone H3 phosphorylation is coupled to poly-(ADP-ribosylation) during reactive oxygen species-induced cell death in renal proximal tubular epithelial cells. *Mol Pharmacol* 60: 394-402, 2001.
37. Waring P, Khan T and Sjaarda A: Apoptosis induced by gliotoxin is preceded by phosphorylation of histone H3 and enhanced sensitivity of chromatin to nuclease digestion. *J Biol Chem* 272: 17929-17936, 1997.
38. Clayton AL and Mahadevan LC: MAP kinase-mediated phosphoacetylation of histone H3 and inducible gene regulation. *FEBS Lett* 546: 51-58, 2003.
39. Lee YJ and Shukla SD: Histone H3 phosphorylation at serine 10 and serine 28 is mediated by p38 MAPK in rat hepatocytes exposed to ethanol and acetaldehyde. *Eur J Pharmacol* 573: 29-38, 2007.
40. Kumar S, Jiang MS, Adams JL and Lee JC: Pyridinylimidazole compound SB 203580 inhibits the activity but not the activation of p38 mitogen-activated protein kinase. *Biochem Biophys Res Commun* 263: 825-831, 1999.
41. Li J, Gorospe M, Hutter D, Barnes J, Keyse SM and Liu Y: Transcriptional induction of MKP-1 in response to stress is associated with histone H3 phosphorylation-acetylation. *Mol Cell Biol* 21: 8213-8224, 2001.
42. Wang D and Lippard SJ: Cisplatin-induced post-translational modification of histones H3 and H4. *J Biol Chem* 279: 20622-20625, 2004.